Estimation of the Frequency and Decay Factor of a Decaying Exponential in Noise

Elias Aboutanios, *MIEEE*

***Abstract*— In this paper we examine the estimation of the parameters of a decaying complex exponential in noise. The strategy adopted consists of a computationally simple two stage scheme where an interpolation stage refines the coarse estimate obtained from an initial maximum bin search. The interpolators of Quinn, and of Aboutanios and Mulgrew, developed for undamped exponentials, are extended to the damped case. In the process we show that Quinn's estimator can be viewed as a linearised version of Bertocco's algorithm. Theoretical analysis demonstrates that the resulting estimators exhibit similar behaviour to the undamped case, leading us to propose two alternative hybrid implemenations that yield a significant improvement in the estimation performance. Unlike the undamped case, however, we discover that a finite number of samples exists for which the estimation performance is best and which we determine in terms of the damping factor. This enables us to adjust the actual number of samples should it deviate significantly from the optimum. Extensive simulation results are presented to support the theoretical findings.**

***Index Terms*— NMR spectroscopy, parameter estimation, DFT interpolation, damped exponential.**

I. I

METABOLOMICS is an important method for characterising fundamental biological processes such as gene expression, disease, drug effects, and toxicity, [1], [2], [3]. Nuclear magnetic resonance (NMR) spectorscopy is a promising technique in Metabolomics for detecting and identifying metabolites, [1], [4]. The free induced decay (FID) signal obtained in NMR spectroscopy is modelled as a sum of decaying exponentials in noise. Thus, the estimation of the parameters of the decaying exponentials is a fundamental step in the processing of NMR spectroscopy signals. This problem is also of prime improtance in many applications such as radar, sonar, speech and biomedical signal processing.

The processing of NMR data, and the estimation of the parameters of damped exponentials in particular, have received some attention in the literature. For a review see [4], and more recently [5] and the references therein. Additionally [6] compiles a relevant and extensive list of references on the wider spectral line analysis problem. Common techniques employed in the NMR context either rely on a long fast Fourier transform (FFT) of the data followed by peak picking, or construct a data matrix from the available data samples which they then process to obtain the required estimates, e.g. [7], [8]. Thus, they incur a significant computational effort. Bertocco, on the other hand, examined this estimation problem and proposed a computationally simple algorithm that relies on a two stage strategy, [9]. In the first stage, a coarse estimate of the frequency is obtained by locating the peak of the FFT of the data sample. An interpolation stage then serves to refine this initial estimate. Helped by the fine stage, Bertocco's algorithm can obtain accurate estimates with a shorter data record than the usual peak picking approach. However, it requires the use of the highly non-linear arc-tangent and logarithm functions, which can be undesirable in certain time-critical applications. Like Bertocco, Umesh and Tufts, presented a method that employs a Newton search for the fine estimation stage, [10]. Their algorithm breaks the two-dimensional search for the frequency and damping factor into two one-dimensional searches. The Newton search, however, has been shown to perform poorly and be prone to numerical problems, [11].

The two-stage estimation strategy has also been used extensively as a solution to the frequency estimation of an undamped complex exponential, [12], [13], [14], [15]. Quinn, [16], proposed a fine interpolation stage that is similar to that of Bertocco as both employ the maximum FFT bin and the two bins either side of it. Unlike Bertocco's algorithm, however, Quinn's interpolator avoids the arc-tangent and logarithmic functions. More recently, Aboutanios and Mulgrew, proposed an iterative interpolation technique that outperform Quinn's algorithm and approaches the Cramer-Rao Bound (CRB), [17]. In this paper, we will focus on simple, fast, and efficient algorithms for the estimation of the parameters of a single complex exponential in noise. In particular, we aim to extend the Quinn, and Aboutanios and Mulgrew (A&M) interpolators to the damped exponential case. In the process, we expose the relationship between Bertocco's and Quinn's algorithms.

Consider the following signal model,

$$x[k] = s[k] + w[k],\ k = 0 \dots N-1, \tag{1}$$

where the signal of interest $s[n]$ is an exponential of the form

$$s[k] = Ae^{(-\eta + j2\pi f)k}. \tag{2}$$

Here A is the complex signal amplitude and η the decay factor. The frequency f is normalised by the sampling frequency, i.e. $f \in [-0.5, 0.5]$. The noise terms, $w[k]$, are zero mean, complex additive white Gaussian with variance σ^2, giving a nominal signal to noise ratio (SNR) $\rho_0 = \frac{|A|^2}{\sigma^2}$. Our goal is to obtain computationally simple, yet robust, estimates of f and η from a block of N samples. The CRBs for the frequency, σ_f^2, and

The author The School of Electrical Engineering and Telecommunications, The University of New South Wales, Building G17, Sydney, NSW, Australia, 2052, phone: +61 2 9385 5010, fax: +61 2 9385 5993 , e-mail: elias@ieee.org..

Parts of this work have been submitted to the IEEE 16th international conference on digital signal processing.

The author would like to thank the anonymous reviewers and Associate Editor for their constructive comments.

damping factor, σ_η^2, were derived in [18] and are given by

$$\begin{aligned}\sigma_\eta^2 &= 4\pi^2\sigma_f^2 \\ &= \frac{(1-e^{-2\eta})^3(1-e^{-2N\eta})}{2\rho_0\left[-N^2e^{-2N\eta}(1-e^{-2\eta})^2+e^{-2\eta}(1-e^{-2N\eta})^2\right]}. \quad (3)\end{aligned}$$

The paper is organised as follows: In section II we consider the noiseless case and derive the various interpolation functions. These algorithms are then analysed in section III where we derive approximate expressions for their estimation variances. Next we examine their iterative implementation in section IV. In section V we evaluate the performance of the algorithms using simulations and discuss their behaviour. Finally, section VI summarises the main conclusions.

II. I A

The discrete time Fourier transform (DTFT) of $s[k]$ is

$$\begin{aligned}X(\lambda) &= \sum_{k=-\infty}^{\infty} s[k]e^{-j2\pi k\lambda} \quad (4)\\ &= A\frac{1-e^{-N\eta+j2\pi N(f-\lambda)}}{1-e^{-\eta+j2\pi(f-\lambda)}}.\end{aligned}$$

The magnitude, $|X(\lambda)|$, exhibits a maximum at $\lambda = f$ given by

$$\max_\lambda |X(\lambda)| = |A|\frac{1-e^{-N\eta}}{1-e^{-\eta}}. \quad (5)$$

Therefore, as in the undamped case, the maximisation of the magnitude spectrum can be used as an estimator of the frequency of the damped sinusoid. However, this maximisation is a computationally expensive and numerically difficult task, which leads us to consider the two stage estimation procedure that relies on the N-point discrete Fourier transform (DFT) of the signal, [9], [10], and which can take advantage of the efficient FFT algorithm. The N-point DFT of the signal is

$$X[n] = A\frac{1-e^{-N\eta+j2\pi(Nf-n)}}{1-e^{-\eta+j\frac{2\pi}{N}(Nf-n)}}.$$

The maximum of $|X[n]|$ now occurs at the index $m = [Nf]$, where $[\bullet]$ indicates the rounding of $\bullet$ to the nearest integer. Now we express the true signal frequency as $f = \frac{m+\delta}{N}$ where $\delta \in [-0.5, 0.5]$ and put $\alpha = N\eta$. The DFT coefficient of the signal at $n = m + p$, henceforth denoted by X_p, becomes

$$X_p = b_p\frac{\alpha - j2\pi\delta}{N\left(1-ze^{\frac{-j2\pi p}{N}}\right)}, \quad (6)$$

where we have put $z = e^{\frac{-\alpha+j2\pi\delta}{N}}$ and defined b_p as

$$b_p = NA\frac{1-e^{-\alpha+j2\pi(\delta-p)}}{\alpha-j2\pi\delta}. \quad (7)$$

Generally, the bulk of the signal's energy is concentrated in just a few DFT coefficients around the maximum bin. Thus, most interpolation algorithms only consider a small number of coefficients around m. The algorithms presented here, focus on the DFT coefficients corresponding to $p = 0, \pm 0.5$, and ± 1. Note that whereas integer p corresponds to DFT bins obtained by the application of the FFT algorithm, a non-integer value necessitates the direct calculaton of the DFT coefficient from the expression in Eq. (4). With this formulation, the estimation of the frequency and damping factor of the signal reduces to the estimation of α and the frequency residual δ. Denoting these estimates by $\hat{\alpha}$ and $\hat{\delta}$, then $\hat{\eta}$ and $\hat{f}$ are calculated as $\hat{\eta} = \frac{\hat{\alpha}}{N}$ and $\hat{f} = \frac{m+\hat{\delta}}{N}$. In what follows we present two interpolation approaches for obtaining these estimates.

A. The Estimators of Bertocco and Quinn

Starting from the DFT expressions, Bertocco proposed an interpolation algorithm that employs the maximum and the two coefficients around it, [9]. Using this same strategy, Quinn presented an estimator of the frequency of an undamped exponential, [16]. As these two algorithms use the same set of DFT coefficients, we treat them together here. We start by reviewing Bertocco's algorithm. We then extend Quinn's estimator to the damped case. This is done in a manner that exposes the relationship between the two approaches.

Let us define the ratio

$$\nu_p = \frac{X_p}{X_0}, \text{ for } p = \pm 1. \quad (8)$$

Noting that $b_{-1} = b_1 = b$ where

$$b = NA\frac{1-e^{-\alpha+j2\pi\delta}}{\alpha-j2\pi\delta}, \quad (9)$$

we substitute the expressions for X_p and X_0 giving

$$\nu_p = \frac{1-z}{1-ze^{-j2\pi\frac{p}{N}}}. \quad (10)$$

Solving for z yields

$$z = \frac{1-\nu_p}{1-\nu_p e^{-j2\pi\frac{p}{N}}}. \quad (11)$$

Therefore, Bertocco suggested that an estimate of z, denoted as $\hat{z}_p$, can be obtained for each value of p. Estimates of the frequency offset and decay factor are then given by

$$\hat{\eta}_p = \frac{\hat{\alpha}_p}{N} = -\ln|\hat{z}_p| \quad \text{and} \quad \hat{\delta}_p = \frac{N}{2\pi}\angle\,\hat{z}_p. \quad (12)$$

At this point a decision has to be made as to which of the two sets of estimates to select. The logical choice is to keep the estimates with the higher SNR. To this end, Bertocco uses the magnitudes $|X_{-1}|$ and $|X_1|$, setting $p = \text{sgn}(|X_1| - |X_{-1}|)$ where sgn($\bullet$) signifies the sign of $\bullet$.

The extension of Quinn's algorithm to the damped case can be done in several ways. Here, we use Bertocco's algorithm as our starting point. This shows that Quinn's algorithm can be viewed as an approximated form of Bertocco's estimator that avoids the arc-tangent and logarithm functions.

Assuming that $\left|\frac{-\alpha+j2\pi\delta}{N}\right| \ll 1$, and $\left|\frac{2\pi p}{N}\right| \ll 1$, we write $z_p^{-1} \approx 1 + \frac{\alpha-j2\pi\delta}{N}$ and $e^{j2\pi\frac{p}{N}} \approx 1 - j2\pi\frac{p}{N}$. Taking the inverse of both sides of Eq. (11) and using these approximations yields

$$1 + \frac{\alpha-j2\pi\delta}{N} \approx \frac{1-\nu_p\left(1-j2\pi\frac{p}{N}\right)}{1-\nu_p}.$$

Simplifying the above expression gives

$$\alpha - j2\pi\delta \approx j2\pi p\frac{\nu_p}{1-\nu_p}.$$

Equivalently, we can write

$$\delta + j\frac{\alpha}{2\pi} \quad \approx \quad h_p \triangleq p\frac{\nu_p}{\nu_p - 1}. \tag{13}$$

Therefore, the real and imaginary parts of h_p can be used as estimators of δ and α respectively. Finally, the estimates of η and δ are found to be

$$\hat{\eta}_p = \frac{\hat{\alpha}_p}{N} = \frac{2\pi}{N}\mathcal{I}(h_p), \quad \text{and} \quad \hat{\delta}_p = \mathcal{R}(h_p), \tag{14}$$

where $\mathcal{R}(\bullet)$ and $\mathcal{I}(\bullet)$ are the real and imaginary parts of $(\bullet)$. This final expression is in effect the same as Quinn's estimator. But here, both the real and imaginary parts of ν_p are required in order to estimate the frequency and damping factor.

As with Bertocco's algorithm, the estimates with the higher SNR are to be selected. Quinn, however, showed that a decision relying on the comparison of the magnitudes of the DFT coeffcients suffers from extremely poor performance as $\delta \to 0$, [11]. Therefore, he proposed setting $p = 1$ if $\hat{\delta}_{-1} \geq 0$ and $\hat{\delta}_1 \geq 0$, otherwise $p = -1$. In what follows, we adopt this decision rule for both Bertocco's and Quinn's algorithms which we group and denote jointly as the (B&Q) algorithm.

B. The A&M Estimator

Quinn's algorithm was analysed in the undamped case and shown to have a frequency dependent performance, [16]. In [17] it was shown that an iterative implementation of Quinn's algorithm results in a degradation in performance due to the interpolation function having its largest variance at the fixed point of the iteration. The A&M estimator, proposed in [17], remedies this handicap and achieves a uniformly lower variance when implemented iteratively. Unlike the B&Q approach, it uses the DFT bins corresponding to $p = \pm 0.5$ and exhibits its best performance at the fixed point. We now adapt the A&M algorithm to the damped exponential case.

Using Eq. (6), we can write for $p = \pm 0.5$

$$X_p \quad = \quad c\frac{\alpha - j2\pi\delta}{N\left(1 - ze^{\frac{-j2\pi p}{N}}\right)}, \tag{15}$$

where we have set

$$c = b_{-0.5} = b_{0.5} = NA\frac{1 + e^{-\alpha + j2\pi\delta}}{\alpha - j2\pi\delta}. \tag{16}$$

Therefore, the interpolation function of the A&M algorithm in the damped case becomes

$$\begin{aligned} h \quad &= \quad \frac{1}{2}\frac{X_{0.5} + X_{-0.5}}{X_{0.5} - X_{-0.5}} \\ &= \quad \frac{j}{2}\frac{1 - z\cos(\frac{\pi}{N})}{z\sin(\frac{\pi}{N})}. \end{aligned} \tag{17}$$

Solving for z yields

$$z = \frac{1}{\cos(\frac{\pi}{N}) - 2jh\sin(\frac{\pi}{N})}.$$

Employing this as an estimator for z, estimates of η and δ can be obtained using (12).

As was done with the B&Q algorithm, a computationally simpler version of the above estimator is now derived. Linearising the DFT expression in Eq. (15) gives

$$X_p \quad = \quad c\frac{\alpha - j2\pi\delta}{\alpha - j2\pi(\delta - p)}. \tag{18}$$

Substituting into the interpolation function of Eq. (17), it is straightforward to show that

$$h \approx \delta + j\frac{\alpha}{2\pi}. \tag{19}$$

Finally, the estimates of δ and η are given by

$$\hat{\eta} = \frac{\hat{\alpha}}{N} = \frac{2\pi}{N}\mathcal{I}(h), \quad \text{and} \quad \hat{\delta} = \mathcal{R}(h). \tag{20}$$

III. A

The asymptotic performances of the Quinn and A&M estimators have been established in [16], [17] for undamped exponentials. In this section, we present theoretical results for the proposed algorithms in the damped case. Including the noise terms into the expression of X_p in (6) yields

$$\tilde{X}_p = b_p\frac{\alpha - j2\pi\delta}{N\left(1 - e^{\frac{-\alpha + j2\pi(\delta - p)}{N}}\right)} + W_p,$$

where W_p are the DFT coefficients of the noise. In the rest of the paper, the noise affected quantities will be denoted by an over∼.

The asymptotic analysis in the undamped case relies on the result that, under some general noise assumptions, $W_p \sim O(\sqrt{N \ln N})$ but $b_p \sim O(N)$, [16], [17]. The damped case, on the other hand, is fundametally different. Although the coefficients W_p maintain the same behaviour, those of the signal do not, for $b_p \to A/(1 - e^{-\eta})$ as $N \to \infty$. In fact, whereas the least squares solution has been shown in [19] to be consistent in the undamped case, no consistent estimation method can be devised for the damped case [20] unless certain strong assumptions are made, [21]. Therefore, no asymptotic analysis is possible here, and we focus on the small sample performance. Assuming a sufficiently high effective SNR, which we define in the following subsection, we make use of the fact that $W_p/b_p \ll 1$ and proceed to derive approximate expressions for the estimation variances.

A. Nominal vs Effective SNR

The estimation performance of the algorithms presented here is a function of the overall or effective SNR of the data record, ρ_{eff}, rather than the nominal SNR, ρ_0. Thus, it is instructive to examine the behaviour of ρ_{eff} as a function of the number of samples as it helps elucidate the analysis and evaluation of the algorithms. To this end, we define ρ_{eff} as the SNR at the true signal frequency, or equivalently the SNR at the true maximum of the periodogram. Putting $p = \delta$ in Eq. (6), the maximum of the periodogram, Y, is given by

$$Y = A\frac{1 - e^{-N\eta}}{1 - e^{-\eta}} + W_\delta.$$

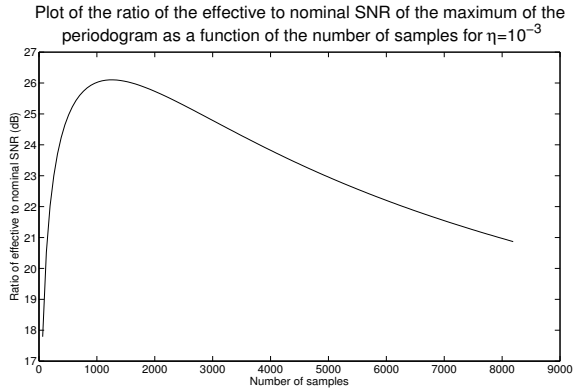

Fig. 1. Ratio of the effective to nominal SNRs, ρ_{eff}/ρ_0, as a function of the number of samples N.

Recalling that the power of the noise coefficient W_δ is $N\sigma^2$, ρ_{eff} can be expressed in terms of the nominal SNR, ρ_0, as

$$\rho_{eff} = \rho_0 \frac{\left(1-e^{-N\eta}\right)^2}{N\left(1-e^{-\eta}\right)^2}. \quad (21)$$

It is easily shown in the undamped case that $\rho_{eff} = N\rho_0$. In the damped case, however, the sample SNR is a decreasing function of the sample number as the signal power decays. Thus, in contrast to the undamped case, ρ_{eff} initially increases as we add more signal, then peaks and starts decreasing as the samples added become dominated by the noise. This is clearly demonstrated in Fig. 1, which shows the ratio ρ_{eff}/ρ_0. Notice that this ratio initially increases as $e^{-N\eta}$ decreases faster than N grows, reaches a maximum then decreases as $e^{-N\eta}$ asymptotes. Notice that for $\eta = 10^{-3}$, ρ_{eff} is still at its maximm point about 25dB higher than ρ_0.

B. Bertocco's and Quinn's Estimators

As Bertocco's estimator was shown to be approximated by the linearised Quinn algorithm, we use the latter as the starting point of our analysis. Substituting Eq. (21) into Eq. (8), and using the assumption $W_p/b \ll 1$, yields

$$\begin{aligned}\tilde{\nu}_p &= \frac{\frac{\alpha-j2\pi\delta}{\alpha-j2\pi(\delta-p)}+\frac{W_p}{b}}{1+\frac{W_0}{b}} \\ &\approx \left(\nu_p+\frac{W_p}{b}\right)\left(1-\frac{W_0}{b}\right) \\ &\approx \nu_p+\frac{W_p}{b}-\nu_p\frac{W_0}{b}. \end{aligned} \quad (22)$$

Let $\xi_p = \tilde{\nu}_p - \nu_p$ and $\epsilon_p = \tilde{h}_p - h_p$. Then

$$\begin{aligned}\epsilon_p &= p\frac{\tilde{\nu}_p}{\tilde{\nu}_p-1} - h_p \\ &= p\frac{\nu_p+\xi_p}{\nu_p+\xi_p-1} - h_p. \end{aligned} \quad (23)$$

Putting $\nu_p = \frac{h_p}{h_p-p}$ into ϵ_p and simplifying gives

$$\begin{aligned}\epsilon_p &= -p\frac{\xi_p(h_p-p)^2}{1+p\xi_p(h_p-p)} \\ &\approx -p\xi_p(h_p-p)^2, \end{aligned} \quad (24)$$

where the last line follows because the assumptions made above imply that $p\xi_p(h_p-p) \ll 1$. Using (22), we substitute the expression for ξ_p into that of ϵ_p and simplify to give

$$\epsilon_p \approx -\frac{p}{b}\Big((h_p-p)W_p - h_pW_0\Big)(h_p-p). \quad (25)$$

Recall that $h_p = \delta + j\frac{\alpha}{2\pi}$. Then, the errors in the estimates of $\eta = \alpha/N$ and δ, denoted by μ and γ respectively, are given by

$$\mu_p = \frac{2\pi}{N}\mathcal{I}(\epsilon_p), \text{ and } \gamma_p = \mathcal{R}(\epsilon_p). \quad (26)$$

Finally, the variances of $\hat{\eta}$ and $\hat{\delta}$, derived in appendix I, become

$$\begin{aligned}\mathrm{Var}[\gamma_p] &= \frac{N^2}{4\pi^2}\mathrm{Var}[\mu_p] \\ &\approx \frac{\alpha^2+4\pi^2\delta^2}{16\pi^4N\rho_0\left[1+e^{-2\alpha}-2e^{-\alpha}\cos(2\pi\delta)\right]}\zeta_p, \end{aligned} \quad (27)$$

where

$$\zeta_p = \alpha^4 + 8\pi^4(|\delta|-1)^2(2\delta^2-2|\delta|+1) + 2\pi^2\alpha^2(4\delta^2-6|\delta|+3).$$

C. A&M Estimator

We now turn to the analysis of the A&M estimator. The DFT coefficients of Eq. (21) for $p = \pm 0.5$ are

$$X_p = c\frac{\alpha-j2\pi\delta}{\alpha-j2\pi(\delta-p)} + W_p. \quad (28)$$

In order to simplify the notation, set $X_+ = X_{0.5}$ and $X_- = X_{-0.5}$. The interpolation function of the A&M estimator becomes

$$\begin{aligned}\tilde{h} &= \frac{1}{2}\frac{X_+ + X_-}{X_+ - X_-} \\ &= \frac{1}{2}\frac{\frac{c}{\alpha-j2\pi(\delta-0.5)}+W_+ + \frac{c}{\alpha-j2\pi(\delta+0.5)}+W_-}{\frac{c}{\alpha-j2\pi(\delta-0.5)}+W_+ - \frac{c}{\alpha-j2\pi(\delta+0.5)}-W_-} \\ &= \frac{\alpha-j2\pi\delta+\frac{\lambda}{2c}(W_++W_-)}{-j2\pi+\frac{\lambda}{c}(W_+-W_-)}, \end{aligned} \quad (29)$$

where

$$\lambda = \alpha^2 - 4\pi^2(\delta^2-0.25) - j4\pi\alpha\delta. \quad (30)$$

Using the assumption that the terms $\left|W_p/c\right| \ll 1$, we obtain

$$\begin{aligned}\tilde{h} &= \frac{1}{-j2\pi}\frac{\alpha-j2\pi\delta+\frac{\lambda}{2c}(W_++W_-)}{1+j\frac{\lambda}{2\pi c}(W_+-W_-)} \\ &\approx \frac{j}{2\pi}\left[\alpha-j2\pi\delta+\frac{\lambda}{2c}(W_++W_-)\right] \\ &\quad\times\left[1-j\frac{\lambda}{2\pi c}(W_+-W_-)\right] \\ &\approx h + j\frac{\lambda}{4\pi c}\left[(1-2h)W_+ + (1+2h)W_-\right]. \end{aligned}$$

Putting $\epsilon = \tilde{h} - h$, and noting that $h = \delta + j\frac{\alpha}{2\pi}$, then μ and γ, which are respectively the errors in η and δ, are given by

$$\mu = \frac{2\pi}{N}\mathcal{I}(\epsilon), \text{ and } \gamma = \mathcal{R}(\epsilon). \quad (31)$$

Finally, the variances of μ and γ, derived in appendix II, are

$$\begin{aligned}\mathrm{Var}[\gamma] &= \frac{N^2}{4\pi^2}\mathrm{Var}[\mu] \\ &\approx \frac{1}{16\pi^4N\rho_0\left[1+e^{-2\alpha}+2e^{-\alpha}\cos(2\pi\delta)\right]}\zeta, \end{aligned} \quad (32)$$

where

$$\begin{aligned}\zeta &= \alpha^6 + 3\pi^2\alpha^4(4\delta^2+1) + \pi^4\alpha^2\left\{48\delta^4 + 8\delta^2 + 3\right\} \\ &\quad +16\pi^6(\delta^2 - 0.25)^2(4\delta^2+1).\end{aligned}$$

The variance expressions have a maximum at $\delta = \pm 0.5$ and minimum at $\delta = 0$. Thus notwithstanding the presence of the damping factor, we expect an iterative implementation of the algorithm to give an improvement in the estimation performance.

IV. I I

The iterative versions of the Quinn and A&M algorithms were shown to converge in the undamped case to the fixed point of the iteration, producing a degradation in the performance of the former and an improvement for the latter, [17]. A close inspection of the variance expressions derived here reveals that the proposed algorithms display similar behaviour to the undamped case and leads us to consider implementing them iteratively.

Let the estimate of δ at the i^{th} iteration be denoted by $\hat{\delta}_i$ and set the initial estimate $\hat{\delta}_0 = 0$. The iterations are constructed as follows: The residual $\hat{\delta}_{i-1}$ is first removed from the signal and the estimator used to give a new estimate $\hat{\delta}_i = \hat{\delta}_{i-1} + \mathcal{R}\left(h(\hat{\delta}_{i-1})\right) = \psi(\hat{\delta}_{i-1})$ where h is the interpolation function. If the procedure is run for Q iterations, then the final estimates become $\hat{\delta}_Q = \psi(\hat{\delta}_{Q-1})$ and $\hat{\eta} = (2\pi/N)\mathcal{I}\left(h(\hat{\delta}_{Q-1})\right)$. This construction is virtually identical to the undamped case, with the only difference occuring at the final iteration where the damping factor is estimated alongside the frequency residual.

At this point we include some statements on the performance of the iterative procedure. Given that no asymptotic analysis is possible, we focus on the case of finite N. The performances of the algorithms, derived in the previous section, imply that the first iteration gives an estimate that is quite close to the true residual. This leaves a remainder to be estimated in the second iteration that is approximately Gaussian with mean 0 and a variance $v \ll 0.5$, meaning that it this residual error is concentrated in a small interval around 0. Consequently, the resulting mean estimation variance will be approximately equal to its value at $\delta = 0$, or more accurately in the immediate vicinity of 0, leading to a significant improvement in the performance of the A&M algorithm and a deterioration in that of the B&Q algorithm.

Now since it is the role of the interpolation function of the first iteration to put the remaining residual close to 0, while the final estimation variance is primarily dependent on the value of the variance due to the subsequent iterations, we propose a hybrid two-iteration implementation that uses Quinn's interpolation function in the first iteration and the A&M estimator in the second. This would result in a computational saving in the first iteration as Quinn's algorithm does not require the calculation of any additional DFT coefficients to those already obtained for the coarse search.

V. R D

The fundamental differences between the estimators presented here and their analogues in the undamped case stem from the presence of α, which encapsulates the combined roles of the damping factor and number of samples, and has implications for the performance. In particular, we will examine the estimation bias and variance, and comment on the selection of the number of samples N.

A. Estimation Bias and Variance

The interpolation functions are biased in the presence of the noise as they are non-linear in the noise coefficients. This is in contrast to the undamped case where the estimators were shown to be asymptotically unbiased. The analysis presented here relies on a high effective SNR condition that ensures $W_p/b \ll 1$ and permits the approximate expressions to be derived. The behaviour of the effective SNR, see Fig. 1, suggests that the estimation performance should have the reverse behaviour, with the bias and variance decreasing, reaching a minimum and then increasing. In fact as N becomes large enough, the effective SNR becomes $\rho_Y \approx \rho_0/N$, indicating that the performance will then deteriorate. It is important, however, to note that the peak in the effective SNR does not necessarily coincide with the lowest estimation bias and variance due to the complicated dependence of these on N.

Although the expected trend in the bias is evident in Figs. 2 and 3, it is important to observe that the biases are much smaller than the CRB. As there are no noticeable differences between the exact and linearised estimators we only show the results of the latter here and in the rest of the manuscript. Additionally, both the A&M and hybrid iterative implementations were run for two iterations and are shown.

The estimation variance is shown in Figs. 4 and 5. Included are the CRB and theoretical performance curves. Both non-iterative (B&Q and A&M) algorithms exhibit the same mean behaviour and are thus represented by the same theoretical mean variance curve. Their differences only emerge when we study them in terms of the residual δ. Note, however, that these differences are significant as they lead to the different iterative behaviour. The theoretical curve obtained by setting $\delta = 0$ in Eq. (32) gives the performance of the iterative algorithms as discussed in section IV and is shown. Now looking at the figures, we see that the performance curves of the interpolators exhibit excellent agreement with the theoretical result. Furthermore, they initially follow the CRB curve down before departing from it, hitting a minimum and then increasing. Also note the improvement of both iterative implementations as they get much closer to the CRB. Finally, the simulations show slightly worse performance of the B&Q algorithm due to the decision step. This impacts the performance of the hybrid algorithm as will become clear later on.

B. Selection of the Number of Samples

The performance results of the previous section clearly show the existence of a value of N for which the estimation variance is minimum. In fact, as we can see from the variance expressions, the dependence of the variance on N and η is summarised by the parameter α. Therefore, we proceed to determine α that gives the minimum variance. This then allows the optimal N to be obtained from η. In the case that no prior

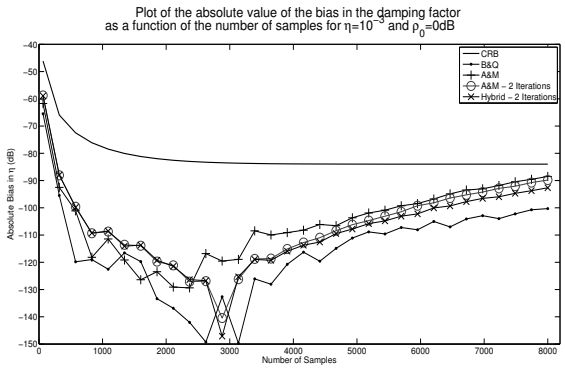

Fig. 2. Plot of the absolute value of the bias in the damping factor as a function of the number of samples N. 10000 Monte Carlo runs were used.

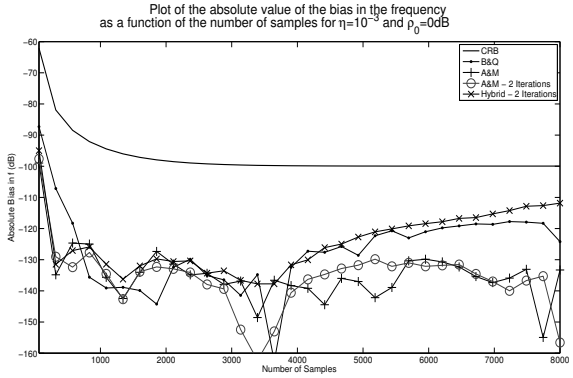

Fig. 3. Plot of the absolute value of the bias in the frequency estimates as a function of the number of samples N. 10000 Monte Carlo runs were used.

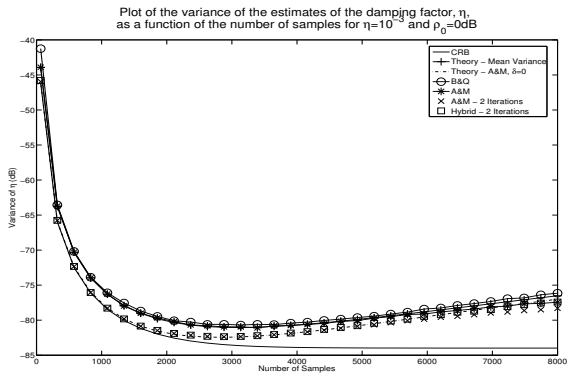

Fig. 4. Plot of the variance of the estimates of the damping factor as a function of the number of samples N. 10000 Monte Carlo runs were used.

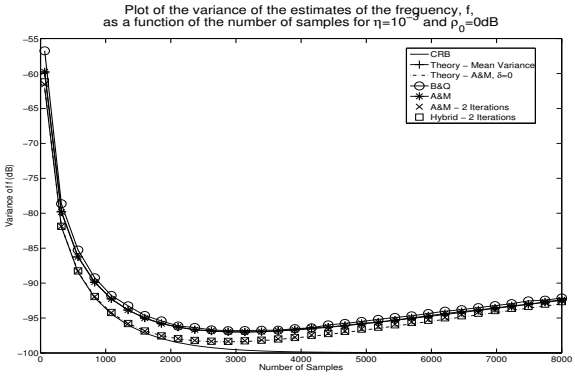

Fig. 5. Plot of the variance of the estimates of the frequency as a function of the number of samples N. 10000 Monte Carlo runs were used.

knowledge on η is available, the initial estimate can be used to adjust the number of samples to improve the performance.

As the non-iterative B&Q and A&M algorithms exhibit the same mean performance as a function of N, we only consider the A&M expression shown in Eq. (32). Assuming δ is uniformly distributed over the interval $[-0.5, 0.5]$, the mean variance as a function of α is proportional to the function

$$q(\alpha) \quad = \quad \int_{-0.5}^{0.5} \frac{\zeta}{\alpha^3 \left[1 + e^{-2\alpha} + 2e^{-\alpha}\cos(2\pi\delta)\right]} d\delta, \quad (33)$$

where ζ is as defined in Eq. (32). The minimum is now found by differentiating $q(\alpha)$ and equating to 0. Solving this numerically, we find that $\alpha \approx 3$. Thus, for $\eta = 10^{-3}$, the lowest variance occurs for $N \approx 3000$ samples, agreeing with the results of the previous section. Now we turn to the iterative algorithms. Let $g(\delta)$ denote the variance expression of the non-iterative A&M algorithm, given in Eq. (32). Then, as it was shown in section IV, the variance of the iterative algorithms converges towards the minimum $g(0)$. Therefore, the optimum value of α for the iterative implemenations is found by setting the derivative of $g(0)$ to 0, which gives $\alpha \approx 2.826$. These two values are quite similar and the performance curve near the optimum is quite flat. In any case, usually a number of samples that is a power of 2 (or some other radix) is used in order to take advantage of efficient implementations of the FFT algorithm. However, being able to determine the optimal N allows us to adjust the number of samples should it be substantially different from the optimum. This certainly can be applied to the iterative implementaton in the second iteration.

C. Estimation Performance Versus the Residual δ and Signal to Noise Ratio

In this section we study the performance of the algorithms as a function of the residual, δ, and nominal SNR, ρ_0. Figs. 6 and 7 give the ratio of the estimation variance to the CRB. In the simulation, we set $N = 1024$ and the SNR $\rho_0 = 0$dB. The figures clearly demonstrate the close agreement between the theory and simulation curves. As expected, the B&Q algorithm has its worst performance at $\delta = 0$ whereas the A&M estimator exhibits a mininum there. The sensitivity of the decision rule to the noise around $\delta = 0$ results in a slight deviation from the theoretical curve of the B&Q and hybrid algorithms. Additionally, the results of the iterative implementations are uniform as a function of the frequency.

The evaluation of the estimators in terms of the SNR is presented in Figs. 8 and 9. The superior performances of the A&M and iterative algorithms are evident. Again visible is the close agreement between the simulation and theoretical results. Note that the B&Q estimator is the worst performing of the algorithms examined in this paper. Also note the breakdown threshold of the algorithms is identical for both the η and f

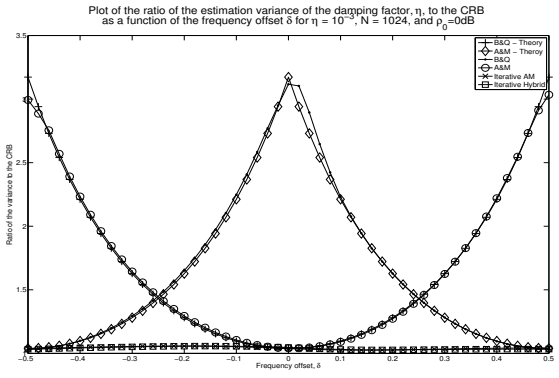

Fig. 6. Ratio of the variance of the damping factor estimates to the CRB as a function of the frequency residual δ. 10000 Monte Carlo runs were used.

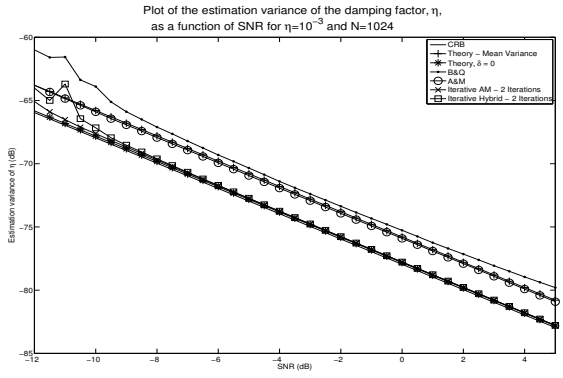

Fig. 8. Plot of the variance of the damping factor estimates as a function of the SNR. 10000 Monte Carlo runs were used.

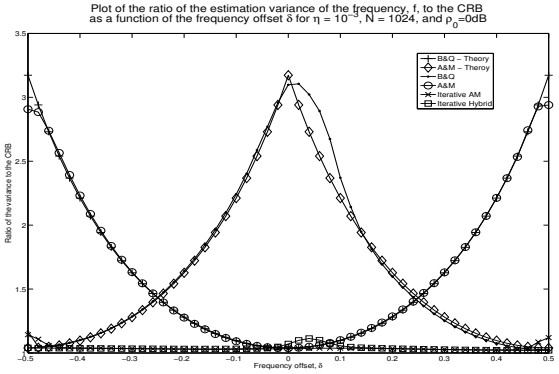

Fig. 7. Ratio of the variance of the frequency estimates to the CRB as a function of the frequency residual δ. 10000 Monte Carlo runs were used.

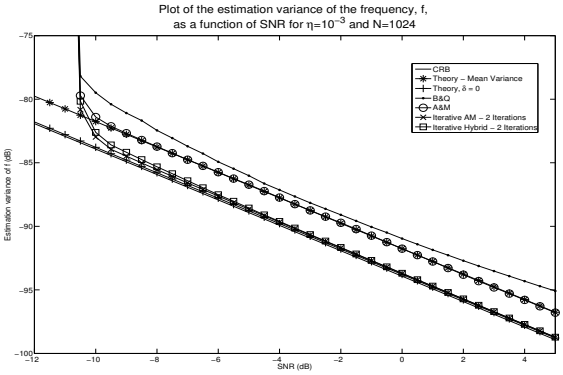

Fig. 9. Plot of the variance of the frequency estimates as a function of the SNR. 10000 Monte Carlo runs were used.

estimators as it stems from the failure of the coarse stage.

Finally we point out that although $\eta = 10^{-3}$ was used in the simulations, the performance trends seen here hold for larger damping factors. However it is important to realise that as η increases, the optimum number of samples decreases according to the result of section V-B. For instance for $\eta = 0.1$, e.g. [10], the optimum number of samples reduces to $N \approx 28$. At this reduced N, the errors in the linearised expressions (due to the linearisation step) may become significant and one may need to employ to exact interpolation expressions for the non-iterative implementations. The iterative implemenations, on the other hand, alleviate this problem as they converge to the vicinity of $\delta = 0$ where the approximation errors are small, thus allowing the approximate interpolation expressions to be used for smaller values of N.

VI. C

Two computationally simple yet robust algorithms for the estimation of the frequency and decay factor of a damped sinusoid in noise are presented and analysed in this work. We extended Quinn's estimator to the damped case and showed that it can be viewed as a linearised version of Bertocco's algorithm. We also derived the interpolation function of the Aboutanios and Mulgrew estimator for this problem. Theoretical analysis of these estimators showed that they exhibit similar behaviour to the undamped case and lead us to consider the iterative implementation of the A&M algorithm. Consequently, we presented two alternative iterative implementations and showed that they produce a significant improvement in the estimation performance. Additionally, in a significant departure from the undamped scenario, the existence of a finite optimal number of samples was proven and its value was obtained as a function of the damping factor. The theoretical performance results were confirmed by simulations.

A I
D A V E
B&Q E

Recall from Eq. (25) that

$$\begin{aligned}\epsilon_p &\approx -\frac{p}{b}\Big((h_p - p)W_p - h_p W_0\Big)(h_p - p)\\ &= -\frac{p}{b}U_p(h_p - p). \end{aligned} \quad (34)$$

Now put $W_p = W_{pR} + jW_{pI}$. Since $h_p = \delta + j\frac{\alpha}{2\pi}$, we have that

$$\begin{aligned}U_p &= U_{pR} + jU_{pI}\\ &= \left[(\delta - p) + j\frac{\alpha}{2\pi}\right]\Big(W_{pR} + jW_{pI}\Big)\\ &\quad -\left(\delta + j\frac{\alpha}{2\pi}\right)(W_{0R} + jW_{0I}) \end{aligned} \quad (35)$$

Next, the real and imaginary parts of U_p become

$$\begin{aligned} U_{pR} &= (\delta - p)W_{pR} - \frac{\alpha}{2\pi}W_{pI} - \delta W_{0R} + \frac{\alpha}{2\pi}W_{0I} \\ \text{and} \\ U_{pI} &= \frac{\alpha}{2\pi}W_{pR} + (\delta - p)W_{pI} - \frac{\alpha}{2\pi}W_{0R} - \delta W_{0I}. \end{aligned}$$

Now substituting into ϵ_p and simplifying yields

$$\epsilon_p \approx -\frac{p}{|b|^2}(b_R - jb_I)\left(Q_{pR} + jQ_{pI}\right),$$

where

$$\begin{aligned} Q_{pR} &= \beta_{p1}W_{pR} - \beta_{p2}W_{pI} - \beta_{p3}W_{0R} + \beta_{p4}W_{0I} \\ \text{and} \\ Q_{pI} &= \beta_{p2}W_{pR} + \beta_{p1}W_{pI} - \beta_{p4}W_{0R} - \beta_{p3}W_{0I}, \end{aligned}$$

and

$$\begin{aligned} \beta_{p1} &= (\delta - p)^2 - \frac{\alpha^2}{4\pi^2}, \\ \beta_{p2} &= \frac{\alpha}{\pi}(\delta - p), \\ \beta_{p3} &= \delta(\delta - p) - \frac{\alpha^2}{4\pi^2}, \text{ and} \\ \beta_{p4} &= \frac{\alpha}{2\pi}(2\delta - p). \end{aligned}$$

Writing $b = b_R + jb_I$, the expressions for μ_p and γ_p become

$$\begin{aligned} \mu_p &\approx -\frac{2\pi}{N}\frac{p}{|b|^2}\left(b_R Q_{pI} - b_I Q_{pR}\right) \\ \text{and} \\ \gamma_p &\approx -\frac{p}{|b|^2}\left(b_R Q_{pR} + b_I Q_{pI}\right). \end{aligned}$$

Recall that the real and imaginary parts of the noise coefficients are i.i.d. with zero mean and variance $N\sigma^2/2$. Then, the variances of μ_p and γ_p can be shown to be approximately

$$\text{Var}[\gamma_p] = \frac{N^2}{4\pi^2}\text{Var}[\mu_p] \approx \frac{N\sigma^2}{2|b|^2}\left(\beta_{p1}^2 + \beta_{p2}^2 + \beta_{p3}^2 + \beta_{p4}^2\right).$$

Replacing $|b|^2$ and β_{p1} - β_{p4} by their expressions and noting that $p\delta = |\delta|$ the variance reduces to the form in Eq. (27).

A II

D A V E

A&M E

Equation (31) implies that the error term ϵ is given by

$$\begin{aligned} \epsilon &\approx j\frac{\lambda}{4\pi c}\left[(1-2h)W_+ + (1+2h)W_-\right] \\ &= j\frac{c^*}{4\pi|c|^2}\lambda U, \end{aligned}$$

where $U = (1-2h)W_+ + (1+2h)W_-$ and λ is given by Eq. (30). Let $W_\pm = W_{\pm R} + jW_{\pm I}$ and $\lambda = \lambda_R + j\lambda_I$, then the real and imaginary parts of U can be shown to be

$$\begin{aligned} U_R &= (1-2\delta)W_{+R} + \frac{\alpha}{\pi}W_{+I} + (1+2\delta)W_{-R} - \frac{\alpha}{\pi}W_{-I} \\ \text{and} \\ U_I &= -\frac{\alpha}{\pi}W_{+R} + (1-2\delta)W_{+I} + \frac{\alpha}{\pi}W_{-R} + (1+2\delta)W_{-I}. \end{aligned}$$

Expanding ϵ we obtain

$$\epsilon \approx \frac{1}{4\pi|c|^2}(c_I + jc_R)(Q_R + jQ_I),$$

with Q_R and Q_I being defined as

$$\begin{aligned} Q_R &= \beta_1 W_{+R} - \beta_2 W_{+I} + \beta_3 W_{-R} + \beta_4 W_{-I} \\ \text{and} \\ Q_I &= \beta_2 W_{+R} + \beta_1 W_{+I} - \beta_4 W_{-R} + \beta_3 W_{-I}, \end{aligned}$$

and

$$\begin{aligned} \beta_1 &= \alpha^2(1-6\delta) - 4\pi^2(1-2\delta)(\delta^2 - 0.25), \\ \beta_2 &= 4\pi\alpha(3\delta^2 - \delta - 0.25) - \frac{\alpha^3}{\pi}, \\ \beta_3 &= \alpha^2(1+6\delta) - 4\pi^2(1+2\delta)(\delta^2 - 0.25), \text{ and} \\ \beta_4 &= 4\pi\alpha(3\delta^2 + \delta - 0.25) - \frac{\alpha^3}{\pi}. \end{aligned}$$

Thus μ and γ become

$$\begin{aligned} \mu &= \frac{2\pi}{N}\mathcal{I}(\epsilon) \approx \frac{1}{2N|c|^2}(c_R Q_R + c_I Q_I) \\ \text{and} \\ \gamma &= \mathcal{R}(\epsilon) \approx \frac{1}{4\pi|c|^2}(c_I Q_R - c_R Q_I). \end{aligned}$$

The variances of μ and γ are then found to be

$$\text{Var}[\gamma] = \frac{N^2}{4\pi^2}\text{Var}[\mu] \approx \frac{N\sigma^2}{32\pi^2|c|^2}\left(\beta_1^2 + \beta_2^2 + \beta_3^2 + \beta_4^2\right).$$

Finally, substituting $|c|^2$ and the expressions for β_1 - $\beta 4$ and simplifying yields the expression shown in Eq. (32).

R

[1] J.L. Griffin, "Metabolic Profiles to Define the Genome: Can We Hear The Phenotypes?," *Phil. Trans. R. Soc. Lond. B, Biological Sciences*, vol. 359, pp. 857–871, 2004.

[2] J.K. Nicholson, J. Connelly, J.C. Lindon, and E. Holmes, "Metabonomics: a Platform for Studying Drug Toxicity and Gene Function," *Nature Reviews Drug Discovery*, vol. 1, pp. 153–161, 2002.

[3] L.M. Raamsdonk, "A functional genomics strategy that uses metabolome data to reveal the phenotype of silent mutations," *Nature Biotechnol*, vol. 19, pp. 45–50, 2001.

[4] R.E. Hoffman and G.C. Levy, "Modern Methods Of NMR Data Processing And Data Evaluation," *Progress in NMR Spectroscopy*, vol. 23, pp. 211–258, 1991.

[5] J.B. Poullet, D.M. Sima, and S. Van Huffel, "MRS signal quantitation: a review of time- and frequency-domain methods," *Journal of Magnetic Resonance*, vol. 195, no. 2, pp. 134–144, 2008.

[6] P. Stoica, "List of references on spectral line analysis," *Signal Processing*, vol. 31, no. 3, pp. 329–340, Apr. 1993.

[7] N. Sandgren, "Parametric methods for frequency-selective MR spectroscopy - a review," *Journal of Magnetic Resonance*, vol. 168, pp. 259272, 2004.

[8] P. Stoica, Y. Selen, N. Sandgren, and S. Van Huffel, "Using prior knowledge in SVD-based parameter estimation for magnetic resonance spectroscopy-the ATP example," *Biomedical Engineering, IEEE Transactions on*, vol. 51, no. 9, pp. 1568–1578, Sept. 2004.

[9] M. Bertocco, C. Offelli, and D. Petri, "Analysis of Damped Sinusoidal Signals via a Frequency-Domain Interpolation Algorithm," *Instrumentation and Measurement, IEEE Transactions on*, vol. 43, no. 2, pp. 245–250, Apr. 1994.

[10] S. Umesh and D.W. Tufts, "Estimation of parameters of exponentially damped sinusoids using fast maximum likelihood estimation with application to NMR spectroscopy data," *Signal Processing, IEEE Transactions on*, vol. 44, no. 9, pp. 2245–2259, Sep 1996.

[11] Barry G. Quinn and E. J. Hannan, *The estimation and tracking of frequency*, Cambridge University Press, New York, 2001.

[12] D. Rife and R. Boorstyn, "Single tone parameter estimation from discrete-time observations," *Information Theory, IEEE Transactions on*, vol. 20, no. 5, pp. 591–598, Sep 1974.
[13] M.D. Macleod, "Fast nearly ML estimation of the parameters of real or complex single tones or resolved multiple tones," *Signal Processing, IEEE Transactions on*, vol. 46, no. 1, pp. 141–148, Jan 1998.
[14] Y.V. Zakharov and T.C. Tozer, "Frequency estimator with dichotomous search of periodogram peak," *Electronics Letters*, vol. 35, no. 19, pp. 1608–1609, Sep 1999.
[15] E. Aboutanios, "A Modified Dichotomous Search Frequency Estimator," *IEEE Signal Processing Letters*, vol. 11, no. 2, pp. 186–188, 2004.
[16] B.G. Quinn, "Estimating frequency by interpolation using Fourier Coefficients," *Signal Processing, IEEE Transactions on*, vol. 42, no. 5, pp. 1264–1268, May 1994.
[17] E. Aboutanios and B. Mulgrew, "Iterative frequency estimation by interpolation on Fourier coefficients," *IEEE Transactions on Signal Processing*, vol. 53, no. 4, pp. 1237–1242, Apr. 2005.
[18] Ying-Xian Yao and S.M. Pandit, "Cramer-Rao lower bounds for a damped sinusoidal process," *Signal Processing, IEEE Transactions on*, vol. 43, no. 4, pp. 878–885, Apr 1995.
[19] C.R. Rao and L.C. Zhao, "Asymptotic behavior of maximum likelihood estimates of superimposed exponential signals," *Signal Processing, IEEE Transactions on*, vol. 41, no. 3, pp. 1461–1464, Mar 1993.
[20] C. Wu, "Asymptotic Theory of Nonlinear Least Squares Estimation," *Annals of Statistics*, vol. 9, no. 3, pp. 501–513, 1981.
[21] D. Kundu, "A Modified Prony Algorithm for Sum of Damped or Undamped Exponential Signals," *Sankhya: The Indian Journal of Statistics*, vol. 56, no. A.3, pp. 524–544, 1994.